DOI: 10.1002/chem.200800771

Protein Nanotubes Comprised of an Alternate Layer-by-Layer Assembly Using a Polycation as an Electrostatic Glue

Xue Qu,[a] Gang Lu,[a] Eishun Tsuchida,*[a] and Teruyuki Komatsu*[a, b]

Abstract: We present the synthesis and structure of various protein nanotubes comprised of an alternate layer-by-layer (LbL) assembly using a polycation as an electrostatic glue. The nanotubes were fabricated by sequential LbL depositions of positively charged polycations and negatively charged proteins into a porous polycarbonate (PC) membrane, followed by release of the cylindrical core by quick dissolution of the template with CH_2Cl_2. This procedure provides a variety of protein nanotubes without interlayer cross-linking. The three-cycle depositions of poly-L-arginine (PLA) and human serum albumin (HSA, $M_w = 66.5$ kDa) into the porous PC template (pore diameter, $D_p = 400$ nm) yielded well-defined $(PLA/HSA)_3$ nanotubes with an outer diameter of 419 ± 29 nm and a wall thickness of 46 ± 8 nm, revealed by scanning electron microscopy (SEM) and transmission electron microscopy (TEM) observations. The outer diameter of the tubules can be controlled by the pore size of the template (200–800 nm), whereas the wall thickness is always constant, independent of the D_p value. The $(PEI/HSA)_3$ (PEI: polyethylenimine) nanotubes showed a slightly thin wall of 39 ± 5 nm. CD spectra of the multilayered $(PEI/HSA)_n$ film on a flat quartz plate suggested that the secondary structure of HSA between the polycations was almost the same as that in aqueous solution. The three-cycle LbL depositions of PLA and ferritin ($M_w = 460$ kDa) or myoglobin (Mb, $M_w = 1.7$ kDa) into the porous PC membrane also gave cylindrical hollow structures. The wall thickness of the $(PLA/ferritin)_3$ and $(PLA/Mb)_3$ nanotubes were 55 ± 5 nm and 31 ± 4 nm; it depends on the globular size of the protein (ferritin > HSA > Mb). The individual ferritin molecule was clearly seen in the tubular walls by SEM and TEM measurements.

Keywords: layer-by-layer assembly · nanotubes · polycations · proteins · supramolecular chemistry

Introduction

Supramolecular templating synthesis using a nanoporous membrane, such as anodic aluminum oxide (AAO) or track-etch polycarbonate (PC), allows construction of well-defined cylindrical hollow structures from a variety of materials.[1–6] In particular, the alternate layer-by-layer (LbL) deposition technique, which is a multilayer build-up onto the pore wall that exploits the electrostatic attraction between oppositely charged molecules, has been widely used for preparation of polyelectrolyte nanotubes.[7–11] The dimensions of the tubes can be determined precisely according to the pore shape interior. Proteins are also natural polyelectrolytes and show versatile bioactivities and biocompatibility. Therefore, the LbL preparation of a protein nanotube has attracted considerable attention because of its potential applications in an enzymatic nanocatalyst,[12a] bioseparation nanofilter,[12b] and targeting nanocarrier.[13] However, there are relatively few reports on liberated protein nanotubes.[14–16] The biomaterial-based LbL assembly has a weak structure. The release of nanotubes from the AAO membrane is commonly achieved by wet chemical etching in aqueous phosphoric acid for several hours. We have previously demonstrated that human serum albumin (HSA) nanotubes prepared in the AAO template easily collapsed in this process unless fixed on a solid substrate.[16] The key point for fabrication of nanotubes by templating synthesis is to remove the cylindrical core from the membrane without damaging it. Martin et al. successfully prepared glucose oxidase and hemoglobin nano-

[a] Dr. X. Qu, Dr. G. Lu, Prof. Dr. E. Tsuchida, Dr. T. Komatsu
Research Institute for Science and Engineering
Waseda University, 3–4–1 Okubo
Shinjuku-ku, Tokyo 169–8555 (Japan)
Fax: (+81) 3-3205-4740
E-mail: eishun@waseda.jp
teruyuki@waseda.jp

[b] Dr. T. Komatsu
PRESTO, Japan Science and Technology Agency (JST)
4–1–8 Honcho, Kawaguchi-shi
Saitama 332–0012 (Japan)

Supporting information for this article is available on the WWW under http://dx.doi.org/10.1002/chem.200800771.

tubes using LbL cross-linking with glutaraldehyde.[14] Although many of them are broken during the collection process, the remaining tubules retained their bioactivities. Nevertheless, some concern remains that polymerization might denature the protein component. Synthesis of protein nanotubes universally without interlayer cross-linking would serve as a trigger to create a new field of bioactive nanotubes.

In this paper, we present the synthesis and structure of various protein nanotubes composed of electrostatic LbL assembly with polycation. The nanotubes were fabricated by alternate LbL depositions of positively charged polycation and negatively charged protein [HSA, ferritin, or myoglobin (Mb)] (Figure 1) into a porous PC membrane, followed by release of the cylindrical core by dissolution of the template with CH_2Cl_2. The effect of the globular size of the protein on the tubular wall thickness has been carefully characterized.

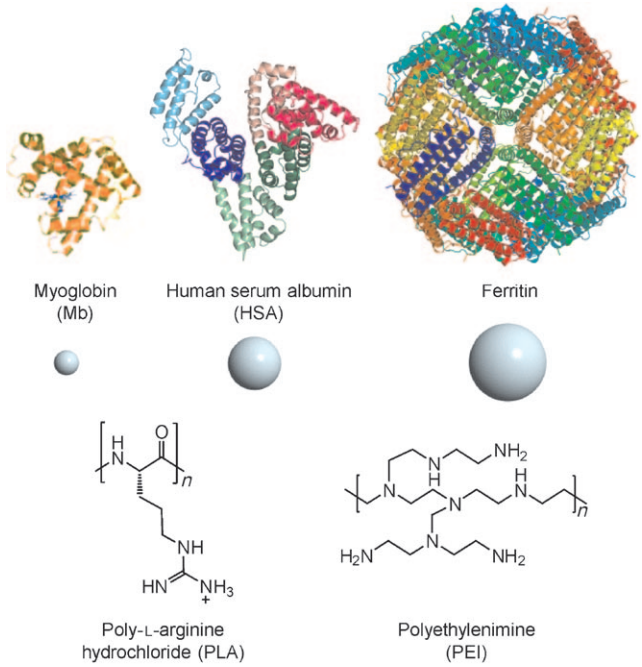

Figure 1. Structures of proteins and polycations used for templating synthesis of nanotubes. The protein pictures were produced based on crystal structure coordinates of Mb (code: 1MBO), HSA (code: 1E78), and ferritin (code: 1IER) using PyMOL (DeLano, W. L. The PyMOL Molecular Graphics System; DeLano Scientific: San Carlos, CA, 2006). The spherical balls depict the relative globular size of the proteins.

Results and Discussion

The most prominent plasma protein in our bloodstream, HSA ($M_w = 66.5$ kDa, $8.0 \times 8.0 \times 3.0$ nm),[17] is negatively charged in a wide range of physiological pH.[18] Phosphate buffered solutions of poly-L-arginine (PLA) and HSA at pH 7.0 were alternately filtered through a porous PC membrane (pore diameter, $D_p = 400$ nm, pore depth: 10 μm) under constant pressure using a syringe pump (Scheme 1).

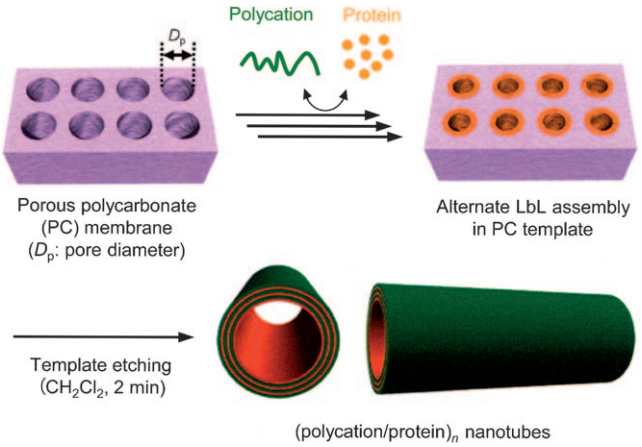

Scheme 1. Preparation of nanotubes by alternate LbL depositions of positively charged polycation and negatively charged protein into porous PC membrane template.

The three-cycle depositions of each component onto the pore wall produced three bilayers of PLA/HSA: $(PLA/HSA)_3$. The adhesive materials on the top and bottom surfaces of the template were removed mechanically by using a cotton swab with water. The resultant membrane was air-dried for 12 h at room temperature. Finally, dissolution of the PC template was achieved by exposure into CH_2Cl_2 solution to release the nanotubes. Other organic solvents, such as acetone, benzene, ethylacetate, and DMSO, were not effective for quick etching of the template. The liberated nanotubes were collected immediately using vacuum filtration.

Scanning electron microscopy (SEM) observations of the filtered sample showed a formation of well-defined hollow cylinders of $(PLA/HSA)_3$ with an outer diameter of 419 ± 29 nm (Figure 2a). The maximum length of the nanotube

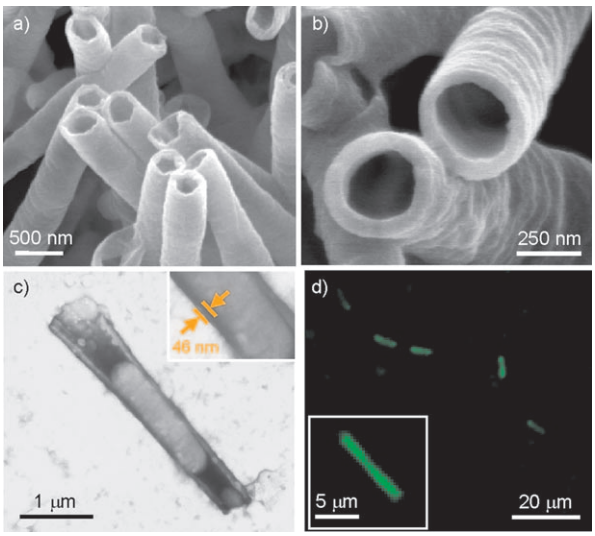

Figure 2. a,b) SEM images and c) TEM images of $(PLA/HSA)_3$ nanotubes. The TEM sample was stained by uranylacetate. d) CLMS images of $(PLA/FITC\text{-}HSA)_3$ nanotubes. These tubules are all prepared by LbL depositions into porous PC template with a $D_p = 400$ nm.

($\approx$9 μm) corresponds to the template thickness. The wrinkles on the outer surface of the tubes are a mirror image of the roughness of the pore wall. Furthermore, shorter nanotubes were also found. These might result from some of the channels in the track-etch PC membrane that do not penetrate the film.[19,20] Interestingly, interconnected channels produced a forked nanotube. Another cause of short tubes might be unexpected defects formed during the alternate LbL assembly at the middle of the pore.

The wall thickness of the $(PLA/HSA)_3$ nanotube was 46 ± 8 nm. The inner diameter was therefore estimated as $\approx$330 nm (Figure 2b). Transmission electron microscopy (TEM) measurements of the tubules on a carbon-coated copper grid elicited identical images to those of SEM observations (Figure 3c); TEM revealed small meniscuses in the

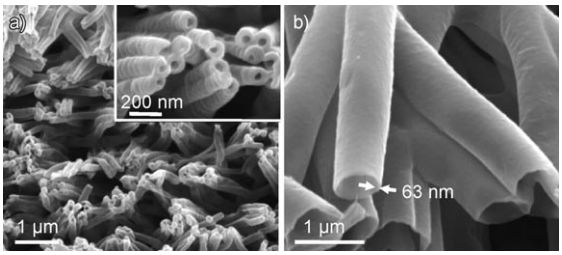

Figure 3. a) SEM images of $(PLA/HSA)_3$ nanotubes prepared by using a 200 nm porous PC template. b) SEM image of $(PLA/HSA)_6$ nanotubes prepared by using a 800 nm porous PC template.

cylinder. When the sample was negatively stained with uranyl acetate (UO^{2+}), the dried nanotube sucked up the aqueous UO^{2+} solution, thereby causing the formation of nanoscale meniscuses. The contact angle of nearly 0° exhibits an extremely hydrophilic internal surface.

The three-cycle LbL depositions of PLA and fluorescein isothiocyanate (FITC) labeled HSA into the 400 nm pore template also yielded identical nanotubes (Figure S1 in the Supporting Information). Confocal laser scanning microscopy (CLSM; Ex at $\lambda=488$ nm) clearly displayed green fluorescing single nanotubes (Figure 2d).

The outer diameter of the $(PLA/HSA)_3$ nanotube can be controlled by the pore size of the PC template used. The three-cycle LbL depositions into the small pore template ($D_p=200$ nm) yielded slender nanotubes with an outer diameter of 154 ± 8 nm (Figure 3a).[21] On the other hand, use of a large pore template ($D_p=800$ nm) produced gigantic tubes with an outer diameter of 708 ± 55 nm.[21] Notably, the wall thicknesses were always constant ($\approx$45 nm), independent of the D_p value. As expected, six-cycle depositions increased the wall thickness to 64 ± 8 nm ($D_p=400$ nm) and 63 ± 7 nm ($D_p=800$ nm) (Figure 3b). They are again independent of the pore size and 1.4-fold larger than that of the three-cycle preparation. Here, we have to be aware that polyelectrolytes swell under aqueous conditions. It appears that the freshly prepared $(PLA/HSA)_6$ is swollen and its thickness is probably double that of wet $(PLA/HSA)_3$. However, after drying, the tubes are shrunk within the pore; thereby, the $(PLA/HSA)_6$ wall became thinner than double the thickness of the dried $(PLA/HSA)_3$. This phenomenon is governed by the degree of swelling of the polyelectrolyte and protein complex.

Li et al. synthesized robust nanotubes by LbL deposition of chitosan and arginate into the porous PC membrane ($D_p=400$ nm) and demonstrated a clear dependence of the wall thickness on the number of deposition cycles: 40 nm at 8 cycles and 80 nm at 16 cycles.[8b] On the other hand, Lee et al. found that the thickness of $(PAH/PSS)_n$ multilayers [PAH: poly(allylamine hydrochloride), PSS: poly(styrene sodium sulfate)] deposited into the nanopore PC template was greater than that of the corresponding flat multilayers on a smooth Si wafer.[10] Increased thickness of bilayers in the pore was similarly observed by Jonas et al. They investigated a pair of strong polyelectrolytes, poly(vinylbenzylammonium chloride) and PSS, with different D_p values.[11] The first bilayer was one or two orders of magnitude thicker (50–120 nm) than that of a corresponding flat bilayer adsorbed onto a Si wafer (1–3 nm), which implies that the small pores are completely filled after only one or two cycle depositions. It is remarkable that the wall thickness in the porous PC template depended on its D_p value. This is, however, inconsistent with our experimental results related to $(PLA/HSA)_n$ nanotubes. In view of these studies, the qualitative molecular mechanism of the LbL assembly of the polyelectrolytes in the porous PC membrane remains unclear. Although the structural formation of the protein/polycation nanotube is also not fully understood, we would presume that the wall thickness of the dried tube reflects the characteristics and size of the protein as well as its packing and orientation in the multilayers.

The three-cycle LbL depositions of polyethylenimine (PEI) and HSA into the porous PC template ($D_p=400$ nm) also yielded well-defined $(PEI/HSA)_3$ nanotubes in which the thickness of the wall (39 ± 5 nm) was slightly less than that of the $(PLA/HSA)_3$ (Figure 4a,b). The six-cycle depositions again led to a 1.5-fold increase in the wall thickness (58 ± 6 nm). Furthermore, we used different polycation as a counterpart to HSA; poly-L-lysine hydrobromide at pH 7.0, PAH at pH 7.0, chitosan hydrochloride at pH 5.0, or HSA at pH 3.8 (under the *p*I value). Unfortunately, no pairing with HSA formed a stable nanotube. The PLA with a strong basic side-chain ($pKa=12.5$)[22] and PEI with highly

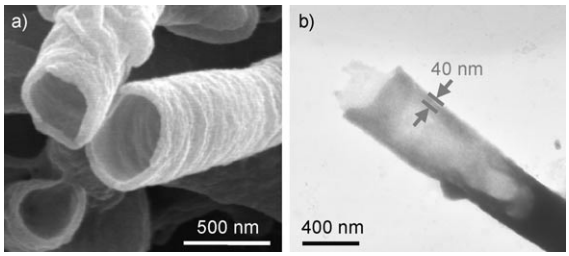

Figure 4. a) SEM image and b) TEM image of $(PEI/HSA)_3$ nanotubes prepared by using a 400 nm porous PC template.

branched structure might be effective for holding the protein layer together as an electrostatic glue in the porous PC membrane.

To characterize the protein structure between the polycations, a LbL $(PEI/HSA)_n$ thin film was prepared on a planar quartz plate using general dipping procedure.[23] The cleaned quartz slide was immersed repeatedly into the PEI and HSA solution, which created multilayers of PEI/HSA. The formation of the alternate LbL assembly was confirmed by using visible absorption spectroscopy. An iron-tetraphenylporphyrin derivative (Figure S2 in the Supporting Information) was incorporated into HSA to enhance the absorption.[24] The initial layer of PEI showed no spectrum in a range of $\lambda = 350$–700 nm. Whereas, the second layer of HSA, laid down on the first PEI film, exhibited intense absorbance at $\lambda = 428$ nm, which is attributed to the Soret band of the incorporated porphyrin. The absorbance at $\lambda = 28$ nm increased linearly with the number of HSA layers, indicating film growth of $(PEI/HSA)_n$ (Figure 5a). The combination of

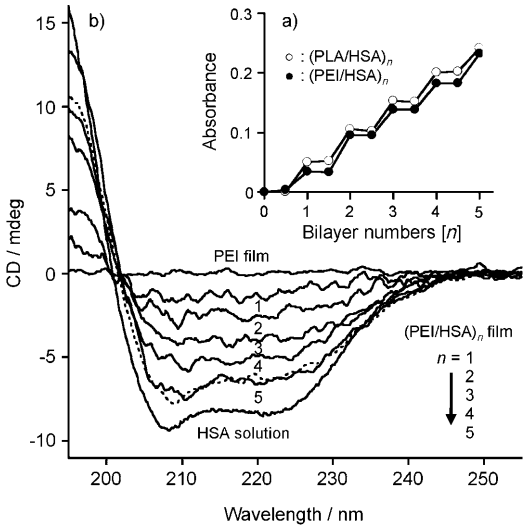

Figure 5. a) UV absorbance at $\lambda = 280$ nm of LbL $(PEI/HSA)_n$ and $(PLA/HSA)_n$ thin film on the planar quartz plate. b) CD spectral changes of LbL $(PEI/HSA)_n$ thin film on the quartz plate (n is the number of the PEI/HSA bilayers). The dashed line is the CD spectrum of the $(PEI/HSA)_5$ film after immersion into CH_2Cl_2 for 5 min.

PLA and HSA also provided a similar LbL assembly. The CD spectra of the obtained $(PEI/HSA)_n$ thin film on the quartz plate showed the same pattern as that of an aqueous solution of HSA (Figure 5b). The negative CD intensities at $\lambda = 208$ and 222 nm decreased in direct relation to the number of bilayers. These results suggest that the secondary structure of HSA between the polycations is probably the same as that in aqueous solution. Moreover, the CD spectrum of the flat $(PEI/HSA)_5$ thin film was absolutely unchanged after immersion into CH_2Cl_2 solution for 5 min. This means that our quick etching procedure of the PC template by exposure into CH_2Cl_2 does not denature the protein.

The stability of the protein nanotube in aqueous solution was also evaluated. The $(PLA/HSA)_3$ nanotubes (outer diameter $= \approx 420$ nm) fixed onto the filter membrane were immersed into water with different pH (7.0, 4.0, and 1.5) and time course of the released HSA content was monitored by measuring the absorbance of the solution at $\lambda = 280$ nm (Figure S3 in the Supporting Information). No significant change was observed in the absorption spectrum at pH 7.0 over a period of 48 h, which indicated that the $(PLA/HSA)_3$ nanotubes were very stable and did not liberate HSA in neutral water. On the other hand, the tubules were deconstructed and released the protein at pH 4.0; approximately 95 % of HSA was dissociated from the tubes within 2 h. The decomposition kinetics accelerated at pH 1.5. The deconstruction of the LbL assembly of PLA/HSA could be caused by the surface charge conversion of HSA at low pH below the pI value (4.8). It suggests that the protein nanotubes can release the proteins in a controlled manner by changing pH value of the solution.

These systematic results for $(PLA/HSA)_n$ nanotubes encouraged further research to fabricate other protein nanotubes. We decided to vary the size of the protein to characterize its effect on the thickness of the tube wall. Ferritin ($M_w = 460$ kDa) is an iron-storage protein comprising 24 identical subunits, which assemble to form a hollow shell with 12 nm diameter.[25] Up to 4,500 iron atoms are stored within this cage as a ferric hydrous oxide phosphate core (8 nm). The three-cycle LbL depositions of PLA and ferritin into the 400 nm PC template yielded well-defined $(PLA/ferritin)_3$ nanotubes with outer diameter of 420 ± 48 nm (Figure 6a). Careful inspection of the SEM images revealed that the wall thickness (55 ± 5 nm) was greater than that of $(PLA/HSA)_3$. To our surprise, plenty of small particles were visible on the surface (Figure 6b); they might be the ferritin molecules under the initial layer of PLA. Magnified pictures

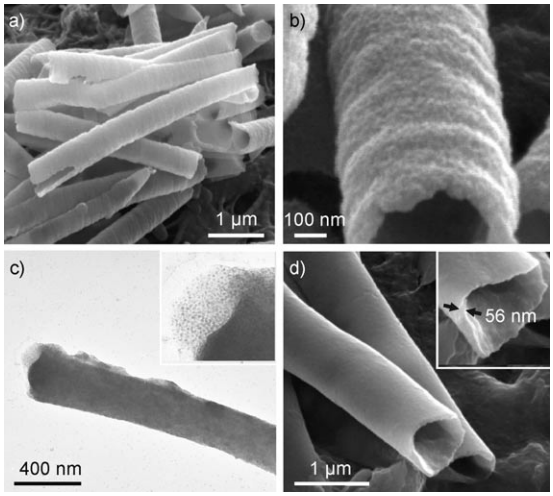

Figure 6. a,b) SEM images and c) TEM images of $(PLA/ferritin)_3$ nanotubes prepared by LbL deposition into porous PC template with a $D_p = 400$ nm. The TEM sample was not stained with contrast agent. d) SEM images of $(PLA/ferritin)_3$ nanotubes prepared using 800 nm porous PC template.

showed the significant differences between the ferritin nanotubes and HSA nanotubes (Figure S4 in the Supporting Information). These unique structural properties are attributed to the large size of the protein. Subsequent TEM measurement of the dried sample without staining clearly revealed the cylindrical shape of the tube caused by the iron mineral core in ferritin (Figure 6c). Under high magnification, the individual iron cluster of 8 nm was detected as small dots in the tubular wall (Figure 6c inset). Elemental analysis of the nanotubes using energy dispersive X-ray (EDX) spectroscopy verified the presence of iron as a component of the structure (Figure S5 in the Supporting Information).

Nanotubes including the dioxygen storage hemoprotein, myoglobin (Mb, $M_w = 17$ kDa, $2.5 \times 3.5 \times 4.5$ nm),[26] were also fabricated in the same manner using PLA and PEI. The respective wall thicknesses of the $(PLA/Mb)_3$ and $(PEI/Mb)_3$ nanotubes were 31 ± 4 nm and 26 ± 4 nm, which are markedly smaller than those of $(PLA/ferritin)_3$, $(PLA/HSA)_3$, and $(PEI/HSA)_3$ (Figure 7a,b). The Mb nanotubes

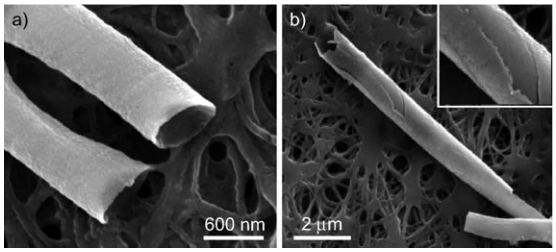

Figure 7. a) SEM image of $(PLA/Mb)_3$ nanotubes and b) SEM images of $(PEI/Mb)_3$ nanotubes. These tubes were prepared by using a 800 nm porous PC template.

were fragile; in some instances, surface layers of the tubules had been partly peeled off (Figure 7b inset). The large ferritin provides a thicker wall and the small Mb confers a thinner wall than that of HSA under the same synthetic protocols. Based on these results, we can conclude that the wall thickness of the protein nanotube is dependent on the globular size of the protein.

Conclusion

Protein nanotubes comprised of an alternate layer-by-layer assembly of human serum albumin, ferritin, and myoglobin with a polycation were prepared by means of a templating synthesis by using a porous PC membrane. The poly-L-arginine and polyethylenimine polycations were effective as an electrostatic glue for holding the protein layer together. The extraction of the nanotube from the template was achieved by immersing the PC membrane into the dichloromethane solution. The protein/polycation nanotubes can be harvested by filtration. It became apparent that the outer diameter of the nanotube can be modulated by the pore diameter of the template and that the tube wall thickness was dependent on the globular size of the protein at the same number of deposition cycles. These cylindrical hollow architectures of proteins will engender development of a new field of smart nanotubes that can be used practically in various applications.

Experimental Section

Materials and apparatus: All reagents were purchased from commercial sources as special grades and were used without further purification. Recombinant human serum albumin (HSA) expressed in *Pichia pastoris*, myoglobin (Mb) from equine skeletal muscle, ferritin from equine spleen, poly-L-arginine hydrochloride (PLA, $M_w = 15{,}000$–$70{,}000$), and HSA-fluorescein isothiocyanate conjugate (FITC-HSA) were purchased from Sigma. Polyethylenimine branched (PEI, $M_w = 25{,}000$) was purchased from Aldrich. The water was deionized by using a Millipore Elix and Simpli Lab-UV. The UV-vis absorption spectra were recorded by using an Agilent 8453 UV-visible spectrophotometer with an Agilent 89090 A temperature control unit. The CD spectra were measured by using a Jasco J-820 circular dichrometer between 195–255 nm.

Templating synthesis of polycation/protein nanotubes: Typically, the $(PLA/HSA)_3$ nanotubes were prepared as follows. The track-etch polycarbonate (PC) membrane (Isopore membrane, $\phi = 25$ mm, $D_p = 400$ or 800 nm; Millipore Corp. or Cyclopore membrane, $\phi = 25$ mm, $D_p = 200$ nm; Whatman Corp.) was fixed into a micro-syringe filter holder (25 mm; Millipore Corp.). The potassium phosphate buffer (p.b.) solution (pH 7.0, 10 mM, 10 mL) of PLA (1 mg mL^{-1}) containing 0.1 M NaCl was injected into the filter using a syringe pump (0.5 mL min^{-1}) to adsorb positively charged PLA onto the pore walls of the PC membrane. Deionized water (10 mL) was then passed through the membrane (1.0 mL min^{-1}) to remove excess PLA and dried under certain vacuum for 10 min. Next, the p.b. solution (pH 7.0, 10 mM, 10 mL) of HSA (2 mg/mL) was filtered the membrane (0.5 mL min^{-1}) to produce a second layer of negatively charged HSA. After washing with water (10 mL, 1.0 mL min^{-1}), the membrane was dried under vacuum (10 min). These pressure infiltrations were repeated for three or six cycles. The positively charged PLA and negatively charged HSA alternately deposit onto the pore surface of the PC membrane to form the electrostatic LbL film of PLA/HSA. The obtained hybrid membrane was rinsed by using deionized water and air-dried for 12 h at room temperature. The top and bottom surfaces of the membrane were wiped carefully using a cotton swab with water to remove the adherent material. Finally, to release the nanotubes, the PC template was dissolved by exposure into a CH_2Cl_2 solution. The liberated nanotubes were collected by vacuum filtration with a tetrafluoroethylene membrane (Omnipore membrane, pore-size 0.1 μm; Millipore Corp.) and washed several times with CH_2Cl_2. Other polycation/protein (PEI/HSA, PLA/Mb, PEI/Mb, ferritin/PLA) nanotubes were fabricated using the same procedure. For these preparations, the p.b. solution (pH 8.5, 10 mM, 10 mL) of Mb (2.0 mg mL^{-1}), p.b. solution (pH 7.0, 10 mM, 10 mL) of ferritin (2.0 mg mL^{-1}), and aqueous solution (10 mL) of PEI (2.0 mg mL^{-1}) containing 0.1 M NaCl were used.

SEM, TEM, and CLSM observations: For SEM measurements, the samples on the Omnipore membrane were sputter-coated with Pd-Pt using a Hitachi E-1045 Ion Sputter. The SEM observations were performed using a Hitachi S-4300 Scanning Electron Microscope operated at an accelerating voltage of 10 kV. For each sample, at least 30 different nanotubes were measured to obtain an average size of outer diameter and wall thickness. For TEM observations, the obtained tubules were redispersed into CH_2Cl_2; a droplet of the solution was placed onto a carbon-coated copper grid (150 mesh), which was lightly hydrophilized by a JEOL Datum HDT-400 hydrophilic treatment device. The dried samples were then stained with aqueous 0.25% uranyl acetate. After removal of the excess fluid using filter paper, the grids were air-dried at room temperature. The obtained specimens were observed using a JEOL JEM-1011 Electron Microscope with accelerating voltage of 100 kV. The EDX spectra were measured by a Gresham/Kevex 6474 detector attached to a

Hitachi H8100 A Electron Microscope. The CLSM measurements were performed by using a Carl Zeiss LSM 510 Laser Scanning Microscope.

Stability evaluations of nanotubes: The dried Omnipore membrane was filtered with the $(PLA/HSA)_3$ nanotube solution and was then cut into pieces and immersed into a p.b. solution (pH 7.0, 10 mM), citric acid buffer solution (pH 4.0, 10 mM), or acidic water (pH 1.5) prepared by addition of HCl (1N). Each solution was incubated at 22 °C accompanied by gentle shaking. The UV absorption spectra of the supernatants were measured at defined time intervals for assay of the free HSA content. The released HSA concentration was calculated from the absorbance at $\lambda = 280$ nm.

Preparations of LbL polycation/protein thin films on planar quartz plate: The quartz plate ($9 \times 35 \times 1$ mm), which had been cleaned by using piranha solution, was first immersed into the aqueous solution of PEI (2 mg mL^{-1}), which contained NaCl (0.1 M) for 10 min to absorb positively charged PEI on the smooth surface. After washing with deionized water three times, the quartz plate was dried with N_2-gas flow for 10 min. The plate was then immersed into the p.b. solution (pH 7.0, 10 mM) of HSA incorporating iron-tetraphenylporphyrin derivative[24] (2 mg mL^{-1}) for 10 min to make a second layer of HSA. This was repeated for several cycles, which engendered formation of multilayered PEI/HSA thin films on the quartz plate. The LbL PLA/HSA film was prepared by using the same procedure.

Acknowledgements

This work was supported by PRESTO "Control of Structure and Functions", JST, Grant-in-Aid for Scientific Research from JSPS (No. 20350058), and Health Science Research Grants from MHLW Japan. Q.X. thanks JSPS Postdoctoral Fellowship for Foreign Researchers.

[1] a) C. R. Martin, L. S. Van Dyke, Z. Cai, W. Liang, *J. Am. Chem. Soc.* **1990**, *112*, 8976–8977; b) C. J. Brumlik, C. R. Martin, *J. Am. Chem. Soc.* **1991**, *113*, 3174–3175; c) C. R. Martin, *Science* **1994**, *266*, 1961–1966; d) S. Hou, C. C. Harrell, L. Tropfin, P. Kohli, C. R. Martin, *J. Am. Chem. Soc.* **2004**, *126*, 5674–5675.

[2] a) M. Steinhart, J. H. Wendorf, A. Greiner, R. B. Wehrspohn, K. Nielsch, J. Schilling, J. Choi, U. Gösele, *Science* **2002**, *296*, 1997–1998; b) M. Steinhart, R. B. Wehrspohn, U. Gösele, J. H. Wendorf, *Angew. Chem.* **2004**, *116*, 1356–1367; *Angew. Chem. Int. Ed.* **2004**, *43*, 1334–1344.

[3] M. Jin, X. Feng, L. Feng, T. Sun, J. Zhai, T. Li, L. Jiang, *Adv. Mater.* **2005**, *17*, 1977–1981.

[4] Y.-G. Guo, J.-S. Hu, H.-P. Liang, L.-J. Wan, C.-L. Bai, *Adv. Funct. Mater.* **2005**, *15*, 196–202.

[5] J. Jang, S. Ko, Y. Kim, *Adv. Funct. Mater.* **2006**, *16*, 754–759.

[6] C. Barret, D. Iacopino, D. O'Carroll, G. de Marzi, D. A. Tanner, A. J. Quinn, G. Redmond, *Chem. Mater.* **2007**, *19*, 338–340.

[7] Z. Liang, A. S. Susha, A. Yu, F. Caruso, *Adv. Mater.* **2003**, *15*, 1849–1853.

[8] a) S. Ai, G. Lu, J. Li, *J. Am. Chem. Soc.* **2003**, *125*, 11140–11141; b) Y. Yang, Q. He, L. Duan, Y. Cui, J. Li, *Biomaterials* **2007**, *28*, 3083–3090.

[9] D. H. Kim, P. Karan, P. Göring, L. Leclaire, A.-M. Caminade, J.-P. Majoral, U. Gösele, M. Steinhart, W. Knoll, *Small* **2005**, *1*, 99–102.

[10] D. Lee, A. J. Nolte, A. L. Kunz, M. F. Rubner, R. E. Cohen, *J. Am. Chem. Soc.* **2006**, *128*, 8521–8529.

[11] H. Alem, F. Blondeau, K. Glinel, S. Demoustier-Champagne, A. M. Jonas, *Macromolecules* **2007**, *40*, 3366–3372.

[12] a) D. T. Mitchell, S. B. Lee, L. Trofin, N. Li, T. K. Nevanen, H. Söderlund, C. R. Martin, *J. Am. Chem. Soc.* **2002**, *124*, 11864–11865; b) S. B. Lee, D. T. Mitchell, L. Trofin, T. K. Nevanen, H. Söderlund, C. R. Martin, *Science* **2002**, *296*, 2918–2200.

[13] S. J. Son, J. Reichael, B. He, M. Schuchman, S. B. Lee, *J. Am. Chem. Soc.* **2005**, *127*, 7136–7317.

[14] S. Hou, J. Wang, C. R. Martin, *Nano Lett.* **2005**, *5*, 231–234.

[15] Y. Tian, Q. He, Y. Cui, J. Li, *Biomacromolecules* **2007**, *7*, 2539–2542.

[16] G. Lu, T. Komatsu, E. Tsuchida, *Chem. Commun.* **2007**, 2980–2982.

[17] A. A. Bhattachrya, S. Curry, N. Frank, *J. Biol. Chem.* **2000**, *275*, 38731–38738.

[18] T. Peter (**1996**) All about Albumin: Biochemistry, Genetics and Medical Applications, Academic Press, San Diego.

[19] P. Apel, *Radiat. Measur.* **2001**, *34*, 559–566.

[20] G. P. Crawford, L. M. Steele, R. Ondris-Crawford, G. S. Iannacchione, C. J. Yeager, J. W. Doane, D. Finotello, *J. Chem. Phys.* **1992**, *96*, 7788–7796.

[21] The average diameter of the pore of the PC template (Isopre membrane or Cyclopore membrane) was measured from SEM image of each template surface; 172 ± 8 nm (Cyclopore, $D_p = 200$ nm), 430 ± 15 nm (Isopore, $D_p = 400$ nm), and 757 ± 14 nm (Isopore, $D_p = 800$ nm). The outer diameters of the isolated nanotubes are consistent with the measured pore size of the templates.

[22] A. P. Ngankam, P. R. Tassel, *Proc. Natl. Acad. Sci. USA* **2007**, *104*, 1140–1145.

[23] Y. Lvov, K. Ariga, I. Ichinose, T. Kunitake, *J. Am. Chem. Soc.* **1995**, *117*, 6117–6123.

[24] T. Komatsu, Y. Matsukawa, E. Tsuchida, *Bioconjugate Chem.* **2002**, *13*, 397–402.

[25] T. Granier, B. Gallois, A. Dautant, B. Langlois d'Estaintot, G. Precigoux, *Acta. Crystallogr., Sec. D* **1997**, *53*, 580–587.

[26] S. E. V. Phillips, *J. Mol. Biol.* **1980**, *142*, 531–554.

Received: April 23, 2008
Published online: September 24, 2008

